

# Azide Conjugatable and pH Responsive Near-Infrared Fluorescent Imaging Probes

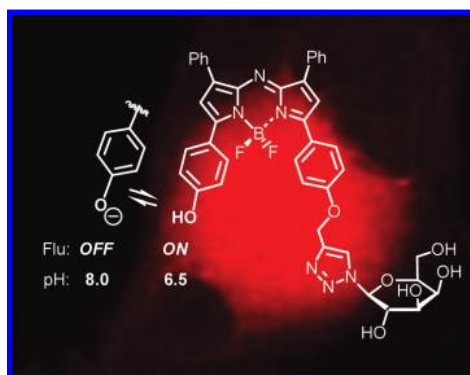
Julie Murtagh, Daniel O. Frimannsson, and Donal F. O'Shea\*

Centre for Synthesis and Chemical Biology, School of Chemistry and Chemical Biology, University College Dublin, Belfield, Dublin 4, Ireland

donal.f.oshea@ucd.ie

Received September 16, 2009

## ABSTRACT



The synthesis and photophysical characteristics of a pH responsive near-infrared fluorescence imaging probe is described. A key feature is the ability to conjugate the probe by an alkyne–azide cycloaddition reaction and its reversible response of fluorescence intensity across the physiological pH range.

The use of high-sensitivity fluorescence imaging as a reporter of in vitro and in vivo molecular processes of biological systems is a powerful research tool.<sup>1</sup> The recent technological advances in noninvasive small animal fluorescence imaging and the future prospect of human fluorescence imaging applications has given rise to a resurgent interest in suitable small molecule fluorophores.<sup>2</sup> In the case of in vivo imaging it is highly preferential to use fluorophores with absorption/emission profiles in the far visible red or near-infrared (NIR) spectral regions (0.7–1.4  $\mu\text{m}$ ), as at lower wavelengths, strong interference from endogenous chromophores is problematic.<sup>3</sup> These stringent spectral requirements have limited such applications to a select few organic fluorophore classes

such as cyanines, squaraines, and seminaphthofluorones.<sup>4–6</sup> In conjunction with optimal photophysical characteristics, two complementary approaches are often adopted to enhance differentiation of the imaging target from background fluorophore. The first, and more common, is the use of conjugated fluorophores generated by the covalent attachment

(3) (a) Ntziachristos, V.; Ripoll, J.; Wang, L. V.; Weissleder, R. *Nat. Biotechnol.* **2005**, *23*, 313. (b) Frangioni, J. V. *Curr. Opin. Chem. Biol.* **2003**, *626*.

(4) For examples see: (a) Lin, Y.; Weissleder, R.; Tung, C.-H. *Bioconjugate Chem.* **2002**, *13*, 605. (b) Citrin, D.; Scott, T.; Sproull, M.; Menard, C.; Tofilon, P. J.; Camphausen, K. *Int. J. Radiat. Oncol. Biol. Phys.* **2004**, *58*, 536. (c) Ballou, B.; Ernst, L. A.; Waggoner, A. S. *Curr. Med. Chem.* **2005**, *12*, 795.

(5) For examples see: Johnson, J. R.; Fu, N.; Arunkumar, E.; Leevy, W. M.; Gammon, S. T.; Piwnica-Worms, D.; Smith, B. D. *Angew. Chem., Int. Ed.* **2007**, *46*, 5528.

(6) Yang, Y.; Lowry, M.; Xu, X.; Escobedo, J. O.; Sibrian-Vazquez, M.; Wong, L.; Schowalter, C. M.; Jensen, T. J.; Fronczek, F. R.; Warner, I. M.; Strongin, R. M. *Proc. Natl. Acad. Sci. U.S.A.* **2008**, *105*, 8829.

(1) Rudin, M.; Weissleder, R. *Nat. Rev. Drug Discovery* **2003**, *2*, 123.

(2) De Grand, A. M.; Frangioni, J. V. *Technol. Cancer Res. Treat.* **2003**, *2*, 1.

of a targeting (bio)-molecule to the fluorescent probe, which facilitates a target-selective accumulation of fluorophore.<sup>7</sup> An alternative approach is the modulation of the fluorescence signal intensity (from low to high) in response to a specific molecular recognition at the endogenous target.<sup>8,9</sup> In spite of the success of both strategies a combination of both processes is rarely investigated. Herein, we outline our strategy to achieve a prototype azide conjugatable and pH responsive NIR fluorescent platform. The on/off fluorescence switching operation would be governed by a straightforward phenol/phenolate interconversion on the fluorophore with conjugation to a molecular targeting motif via an alkyne–azide cycloaddition. To date, there are few literature reports of NIR pH responsive fluorophores in spite of their potential imaging applications for disease states that can induce localized intra- and extracellular pH changes such as cancers, renal failure, and ischemia.<sup>10</sup> Recently, pH responsive cyanine fluorophores covalently attached to bacteriophage particles have been reported.<sup>11</sup>

We have recently developed the BF<sub>2</sub>-chelated tetraaryl-lazadipyrrromethene fluorophore class **1** with excellent absorption and fluorescence properties in the 650–750 nm spectral region.<sup>12</sup> For example, the tetraaryl analogue **1** has an absorption  $\lambda_{\text{max}}$  at 688 nm ( $\epsilon = 85\,000\text{ dm}^{-3}\text{ mol}^{-1}\text{ cm}^{-1}$ ) and emission at 716 nm ( $\phi_{\text{F}} = 0.36$ ) in chloroform (Figure 1). These promising photophysical characteristics have

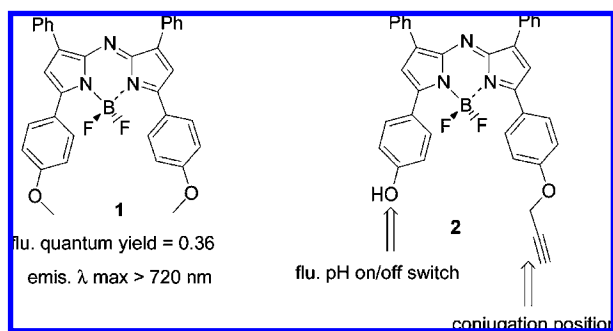


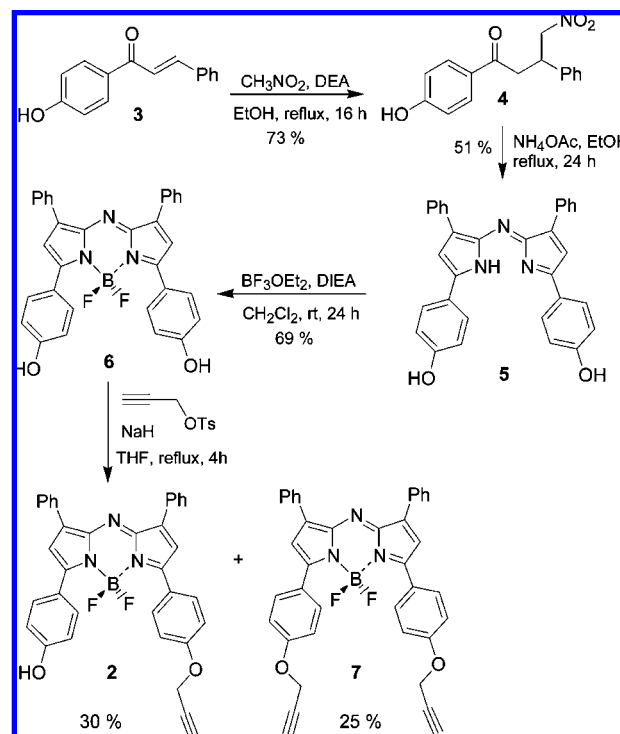
**Figure 1.** BF<sub>2</sub>-chelated tetraaryl-lazadipyrrromethenes.

encouraged the adaption of this class to specific functions such as fluorescent sensors<sup>13</sup> and photodynamic therapeutic agents.<sup>14</sup> The synthetic strategy adopted for our current goal was to develop a short route to the monoalkyne-monophenol-substituted analogue **2** (Figure 1). It was anticipated that **2**

would be capable of conjugation via azide cycloaddition and the intensity of fluorescence output would be controlled by a phenol/phenolate interconversion.

The synthetic route commenced with an addition of nitromethane to chalcone **3**, which gave 1-(4-hydroxyphenyl)-4-nitro-3-phenylbutan-1-one **4** in 73% yield (Scheme 1). Subsequent generation of the bis-phenol-substituted

**Scheme 1.** Synthesis of Fluorophore **2**



azadipyrrromethene **5** was achieved by the reflux of **4** with ammonium acetate in ethanol for 24 h. Filtration of the precipitate from the crude reaction mixture gave the pure product in 51% yield. Compound **5** was converted to its BF<sub>2</sub>-chelated analogue **6** with BF<sub>3</sub> diethyletherate and diisopropylethylamine (DIEA) in dichloromethane for 24 h. An

(7) For examples see: (a) Citrin, D.; Lee, A. K.; Scott, T.; Sproull, M.; Menard, C.; Tofilon, P. J.; Camphausen, K. *Mol. Cancer Ther.* **2004**, *3*, 481. (b) Petrovsky, A.; Schellenberger, E.; Josephson, L.; Weissleder, R.; Bogdanov, A. *Cancer Res.* **2003**, *63*, 1936. (c) Ramjiawan, B.; Maiti, P.; Aftanas, A.; Kaplan, H.; Fast, D.; Mantsch, H. H.; Jackson, M. *Cancer* **2000**, *89*, 1134.

(8) Rao, J.; Dragulescu-Andrasi, A.; Yao, H. *Curr. Opin. Biotechnol.* **2007**, *18*, 17.

(9) (a) Fonović, M.; Bogoy, M. *Curr. Pharm. Des.* **2007**, *13*, 253. (b) Blum, G.; Mullins, S. R.; Keren, K.; Fonovic, M.; Jedeszko, C.; Rice, M. J.; Sloane, B. F.; Bogoy, M. *Nat. Chem. Biol.* **2005**, *1*, 203.

(10) (a) Gillies, R. J.; Raghunand, N.; Garcia-Martin, M. L.; Gatenby, R. A. *IEEE Eng. Med. Biol. Mag.* **2004**, *23*, 57. (b) Stubbs, M.; McSheehy, P. M. J.; Griffiths, J. R.; Bashford, C. L. *Mol. Med. Today* **2000**, *6*, 15.

(11) (a) Hilderbrand, S. A.; Kelly, K. A.; Niedre, M.; Weissleder, R. *Bioconjugate Chem.* **2008**, *19*, 1635. (b) Zhang, Z.; Achilefu, S. *Chem. Commun.* **2005**, 5887.

(12) (a) Gorman, A.; Killoran, J.; O'Shea, C.; Kenna, T.; Gallagher, W. M.; O'Shea, D. F. *J. Am. Chem. Soc.* **2004**, *126*, 10619. (b) Killoran, J.; Allen, L.; Gallagher, J. F.; Gallagher, W. M.; O'Shea, D. F. *Chem. Commun.* **2002**, 1862.

(13) (a) Killoran, J.; McDonnell, S. O.; Gallagher, J. F.; O'Shea, D. F. *New J. Chem.* **2008**, 483. (b) Loudet, A.; Bandichhor, R.; Wu, L.; Burgess, K. *Tetrahedron* **2008**, *64*, 3642. (c) Gawley, R. E.; Mao, H.; Mahbubul Haque, M.; Thorne, J. B.; Pharr, J. S. *J. Org. Chem.* **2007**, *72*, 2187. (d) Killoran, J.; O'Shea, D. F. *Chem. Commun.* **2006**, 1503. (e) Hall, M. J.; Allen, L. T.; O'Shea, D. F. *Org. Biomol. Chem.* **2006**, *4*, 776. (f) McDonnell, S. O.; O'Shea, D. F. *Org. Lett.* **2006**, *8*, 3493.

(14) (a) McDonnell, S. O.; Hall, M. J.; Allen, L. T.; Byrne, A.; Gallagher, W. M.; O'Shea, D. F. *J. Am. Chem. Soc.* **2005**, 16360. (b) Gallagher, W. M.; Allen, L. T.; O'Shea, C.; Kenna, T.; Hall, M.; Killoran, J.; O'Shea, D. F. *Br. J. Cancer* **2005**, *92*, 1702. (c) Byrne, A. T.; O'Connor, A.; Hall, M.; Murtagh, J.; O'Neill, K.; Curran, K.; Mongrain, K.; Rousseau, J. A.; Lecomte, R.; McGee, S.; Callanan, J. J.; O'Shea, D. F.; Gallagher, W. M. *Br. J. Cancer* **2009**, *101*, 1565.

isolated yield of 69% was obtained following chromatography on silica gel. The synthesis of our target compound **2** required a desymmetrization step involving alkylation of one of the two phenol groups.<sup>15</sup> This alkylation was carried out with 2.2 equiv of propargyl-tosylate and NaH in THF for 4 h under reflux. It was found that these specific conditions biased the distribution of mono-**2** and bis-alkylated **7** products toward the mono-substituted derivative (Scheme 1). Exploiting the large polarity difference between **2** and **7** allowed for facile separation on silica gel chromatography and gave products in isolated yields of 30% and 25%, respectively.

Spectral properties of **2** in organic solvents were very similar to those of **1** with the absorption and emission maxima of **2** in CHCl<sub>3</sub> at 680 and 708 nm, respectively, with a high fluorescence quantum yield ( $\Phi_f$ ) of 0.37 (Table 1,

**Table 1.** Absorption/Emission Properties of **2**

entry	solvent	$\lambda_{\max}$ abs (nm) <sup>a</sup>	$\lambda_{\max}$ flu (nm) <sup>b</sup>
1	CHCl <sub>3</sub>	680	708 <sup>c,d</sup>
2	C <sub>7</sub> H <sub>8</sub>	685	711
3	CH <sub>3</sub> OH	688	716
4	H <sub>2</sub> O/CrEL	700	729

<sup>a</sup>  $5 \times 10^{-6}$  M. <sup>b</sup>  $5 \times 10^{-7}$  M. <sup>c</sup>  $\Phi_f = 0.37$  (**1** as standard). <sup>d</sup> Addition of DBU resulted in a 75-fold reduction of fluorescence intensity (SI).

entry 1, SI). Spectral characteristics showed a slight dependence upon solvent dipolarity with bathochromatic shifts of 8 nm for absorbance and emission maxima in methanol (Table 1, entry 3, SI). Additionally, an aqueous solution generated by formulation using Cremophor EL<sup>12a</sup> showed further small bathochromic shifts (700/729 nm) when compared to organic solvents (entry 4, SI).

In contrast to **1**, the spectral properties of **2** displayed a striking response across the physiological pH range (Figure 2). The excited state response of **2** at the  $\lambda_{\max}$  of 729 nm in

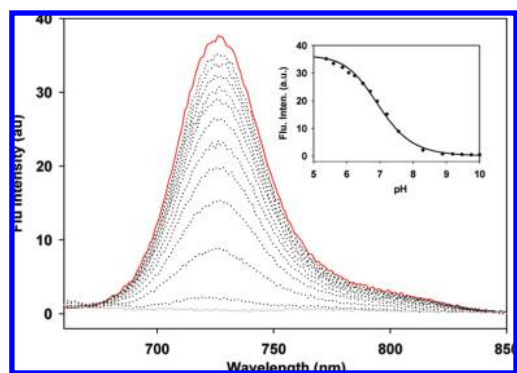
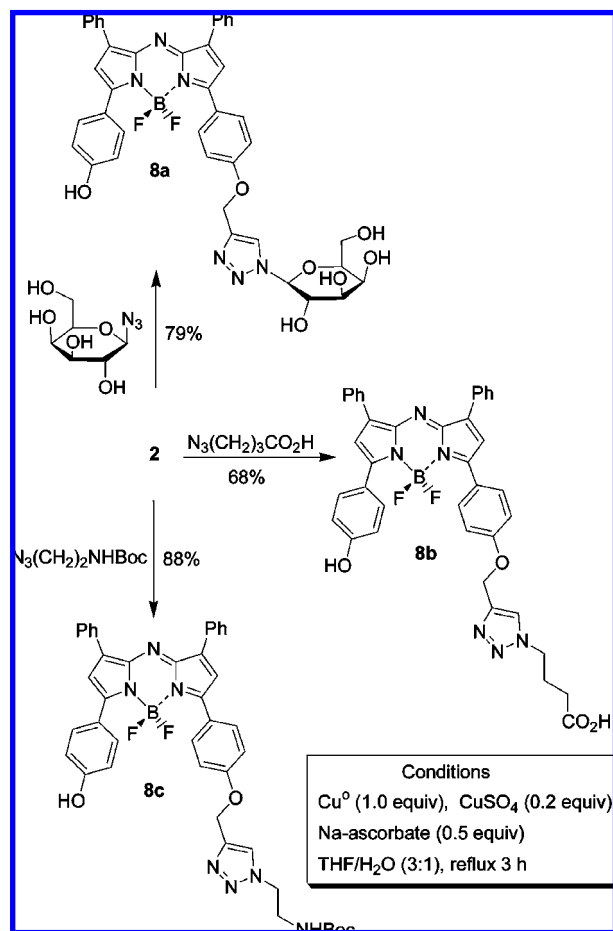


**Figure 2.** pH responsive fluorescence spectra of **2**: red trace, pH 6.0; gray trace, pH 9.0. Excitation at 640 nm, slit widths 10 nm,  $5 \times 10^{-7}$  M in water/CrEL.  $I_{\text{NaCl}} = 150$  mmol/L. Inset: Sigmoidal plot predicting a  $pK_a$  value of 6.9.

aqueous solutions showed a greater than 15-fold fluorescence intensity differential between pH 6 and 8 with virtually complete suppression of fluorescence signal at pH 9 (Figure 2). A sigmoidal plot of pH versus fluorescence intensity predicted an apparent  $pK_a$  of 6.9 (Figure 2, inset).<sup>16</sup> As would be expected for an ICT process, the UV–visible spectrum of **2** was strongly influenced by pH. The absorption band at 700 nm was progressively reduced in intensity with increasing pH and a new band appeared at 775 nm with an isosbestic point at 740 nm indicative of the formation of a monodeprotonated species (SI).

The mild aqueous conditions required for azide–alkyne cycloadditions offer distinct advantages when utilized for bioconjugation reactions.<sup>17</sup> To demonstrate functional group tolerance of azide reactions with **2**, three azides containing amino, carboxy, and carbohydrate substituents were tested. The optimized reaction conditions with 1-azido-1-deoxy- $\beta$ -D-galactopyranoside, 4-azidobutyric acid, and (2-azidoethyl)carbamic acid *tert*-butyl ester were identified as CuSO<sub>4</sub>/Cu/sodium ascorbate in THF/H<sub>2</sub>O (3:1) under reflux for 3 h (Scheme 2). The copper salts were removed by aqueous

**Scheme 2.** Azide Cycloaddition Reactions



extraction and cycloadducts **8a–c** were isolated in good yields of 68% to 88% following either recrystallization from methanol or column chromatography.

We were pleased to observe that the UV–vis/fluorescence spectra of **8a–c** in methanol showed little difference from each other or from the alkyne derivative **2** demonstrating that the cycloaddition reaction had negligible effect on these spectral characteristics (Figure 3). As a representative example, the pH

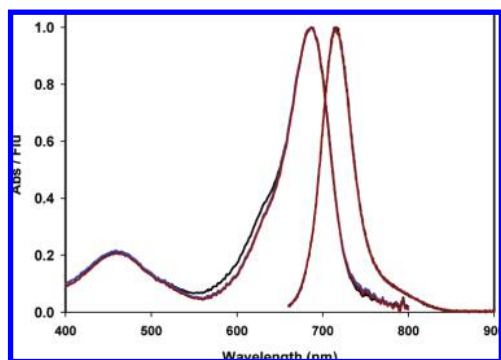


**Figure 3.** Normalized UV–vis ( $5 \times 10^{-6}$  M) and fluorescence ( $5 \times 10^{-7}$  M) spectra of **8a** ( $\lambda_{\text{max}}$  687/716 nm; brown), **8b** ( $\lambda_{\text{max}}$  687/716 nm; black), and **8c** ( $\lambda_{\text{max}}$  687/716 nm; blue) in MeOH.

responsive nature of the galactose conjugated derivative **8a** was examined and shown to have similar ground and excited state responses as that of **2** with  $pK_a$  of 6.9 (SI). Analysis of the fluorescence intensity of **8a** at five different pH values illustrated how a significant bias toward higher fluorescence intensity at low physiological pH regions was accomplished. For example, comparison of the measured fluorescence intensity difference from pH 6.1 to 7.2 was greater than 2-fold and the difference between pH 6.6 and 8 was 6-fold (Figure 4).

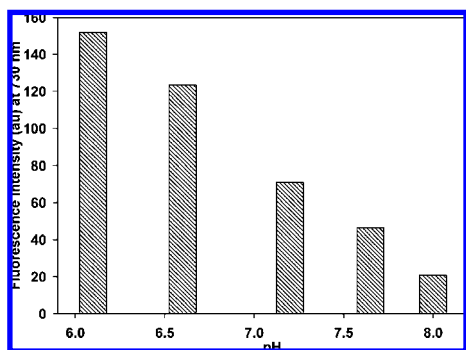


**Figure 4.** Relative fluorescence intensity at 730 nm of **8a** at pH 6.1, 6.6, 7.2, 7.6, and 8.0. Excitation at 640 nm, slit widths 20 nm,  $5 \times 10^{-7}$  M in water/CrEL.  $I_{\text{NaCl}} = 150$  mmol/L.

Demonstration of cell internalization and in vitro pH response of **8a** was achieved by incubation with MDA-MB-

231 cells for 1 h followed by blue nuclear costaining with 4,6-diamidino-2-phenylindole (DAPI). Dual-color imaging with confocal laser scanning microscopy (CLSM) showed a distinct red emission from **8a** localized to the cytosol (SI).

Illustrative reversible on/off switching of intracellular **8a** could be achieved by treating a population of dual-stained cells with aqueous carbonate buffer of pH 8.0 or acidic buffer of pH 6.6 (Figure 5, SI). Imaging of the same cell population

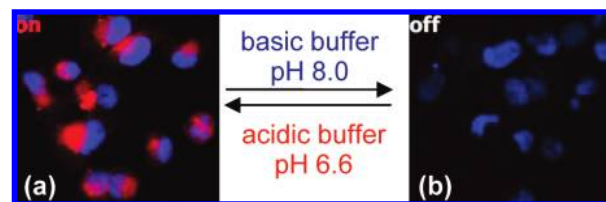


**Figure 5.** CLSM images of **8a** (red) with fixed MDA-MB-231 cells costained with nuclear stain DAPI (blue). Cell population imaged following treatment with (a) pH 6.6 buffer and (b) pH 8.0 buffer.

following addition of basic buffer showed almost complete quenching of the red emission of **8a** with the blue nuclear DAPI emission still clearly visible. In contrast, following the addition of pH 6.6 buffer to the cells the emission from **8a** was re-established. The difference in averaged whole cell red fluorescence taken from off-cells to on-cells was 6-fold.

In summary, an efficient synthesis, photophysical characteristics, and intracellular demonstration of a new pH responsive fluorochrome platform with emission at 730 nm is outlined. The noninvasive in vivo imaging potential of bioconjugated derivatives of **2** is currently under investigation and will be described in due course.

**Acknowledgment.** Funding support from Science Foundation Ireland is gratefully acknowledged. The authors thank the CSCB Mass Spectrometry and NMR Centres.

**Supporting Information Available:** All experimental procedures and spectra. This material is available free of charge via the Internet at <http://pubs.acs.org>.

OL902140V

(15) For an alternative synthetic approach to unsymmetrical derivatives see: Hall, M. J.; McDonnell, S. O.; Killoran, J.; O'Shea, D. F. *J. Org. Chem.* **2005**, *70*, 5571.

(16)  $pK_a$  values in a micellar microenvironment are often lower than anticipated.

(17) For recent examples see: (a) Laughlin, S. T.; Baskin, J. M.; Amacher, S. L.; Bertozzi, C. R. *Science* **2008**, *320*, 664. (b) Gramlich, P. M. E.; Warnche, S.; Gierlich, J.; Carell, T. *Angew. Chem., Int. Ed.* **2008**, *47*, 3442. (c) Mindt, T. L.; Struthers, H.; Brans, L.; Anguelov, T.; Schweinsberg, C.; Maes, V.; Tourwé, D.; Schibli, R. *J. Am. Chem. Soc.* **2006**, *128*, 15096. (d) Casas-Solvas, J. M.; Vargas-Berenguel, A.; Capitán-Vallvey, L. F.; Santoyo-González, F. *Org. Lett.* **2004**, 3687.